ARTICLE IN PRESS
YICAR:8714
Icarus ••• (••••) •••–•••
Contents lists available at ScienceDirect
Icarus
www.elsevier.com/locate/icarus

Near-Earth asteroid surface roughness depends on compositional class

Lance A.M. Benner [a,*], Steven J. Ostro [a], Christopher Magri [b], Michael C. Nolan [c], Ellen S. Howell [c], Jon D. Giorgini [a], Raymond F. Jurgens [a], Jean-Luc Margot [d], Patrick A. Taylor [d], Michael W. Busch [e], Michael K. Shepard [f]

[a] *Jet Propulsion Laboratory, California Institute of Technology, 4800 Oak Grove Drive, Pasadena, CA 91109, USA*
[b] *University of Maine at Farmington, 173 High Street, Preble Hall, Farmington, ME 04938, USA*
[c] *Arecibo Observatory, HC3 Box 53995, Arecibo, PR 00612, USA*
[d] *Department of Astronomy, Cornell University, Ithaca, NY 14853, USA*
[e] *Division of Geological and Planetary Sciences, California Institute of Technology, Pasadena, CA 91125, USA*
[f] *Department of Geography and Geosciences, Bloomsburg University, Bloomsburg, PA 17815, USA*

ARTICLE INFO

Article history:
Received 21 February 2008
Revised 18 June 2008

Keywords:
Near-Earth objects
Asteroids
Asteroids, surfaces
Asteroids, composition
Radar observations

ABSTRACT

Radar observations of 214 near-Earth asteroids (NEAs) reveal a very strong correlation of circular polarization ratio with visible–infrared taxonomic class, establishing distinct differences in the centimeter-to-several-decimeter structural complexity of objects in different spectral classes. The correlation may be due to the intrinsic mechanical properties of different mineralogical assemblages but also may reflect very different formation ages and collisional histories. The highest ratios are measured for groups associated with achondritic igneous rocky meteorites: the E class, whose parent body may be 3103 Eger, and the V class, derived from the mainbelt asteroid (and Dawn mission target) 4 Vesta.

1. Introduction

Meteorites are samples of small, Earth-orbit-crossing asteroids, which in turn are primarily derived from the main asteroid belt (Burbine et al., 2002; Lipschutz and Schultz, 2007). The mineralogy and meteoritic analogues of asteroids are constrained by narrow-band optical reflectance spectra (Tholen and Barucci, 1989; Bus et al., 2002) and to a lesser extent by classification schemes based on broadband optical color indices and albedos (Burbine et al., 2002; Lipschutz and Schultz, 2007). Asteroid classification schemes now include some 26 spectral classes (Bus et al., 2002), in most cases tentatively associated with meteorite types (Burbine et al., 2002; Lipschutz and Schultz, 2007). A dependence of the abundance of different spectral classes on heliocentric distance (Gradie and Tedesco, 1982) probably reflects the influence of temperature on the identity of condensates from the primitive solar nebula. However, there remains great uncertainty in the relationships between meteorite types and asteroid classes. The rare exceptions involve asteroids visited by rendezvous spacecraft: the ∼15-km-diameter NEA 433 Eros (Veverka et al., 1997) and the several-hundred-meter-long NEA 25143 Itokawa (Fujiwara et al., 2006) are both mineralogically akin to ordinary chondrites. Similarly, there is only limited information about the physical characteristics of NEA surfaces, which are the outcome of complex collisional histories and reflect the mechanical properties of objects' mineral assemblages.

A radar echo's circular polarization ratio measures the wavelength-scale roughness of the target's surface (Ostro et al., 2002; Ostro, 2007). In almost all radar observations, a circularly polarized signal is transmitted and the echo is measured simultaneously in the same sense of circular polarization as transmitted (the SC sense) and the opposite (OC) sense. The handedness of a circularly polarized signal is reversed upon reflection from a smooth dielectric interface, leading to dominance of the echo by the OC polarization. Multiple scattering, subsurface reflection, wavelength-scale facets, and structure with radii of curvature near the wavelength can produce SC echoes. Therefore, the SC/OC ratio is a measure of the near-surface, wavelength-scale structural complexity or "roughness." Since the sensitivities of the two polarization channels are easily calibrated via measurement of unpolarized radio sources, the uncertainty in SC/OC estimates is limited to the propagation of statistical fluctuations in receiver noise. To place the results below in context, Mercury, Venus, and the Moon have SC/OC ∼ 0.1 and Mars has a ratio of about 0.3, although for each object, there are local variations.

2. Results

Here we report 3.5- and 13-cm-wavelength radar observations of 214 near-Earth asteroids (Figs. 1, 2; Tables 1, 2, and 3) that reveal a very strong correlation between circular polarization ratio

* Corresponding author. Fax: +1 818 354 9476.
E-mail address: lance.benner@jpl.nasa.gov (L.A.M. Benner).

0019-1035/$ – see front matter
doi:10.1016/j.icarus.2008.06.010

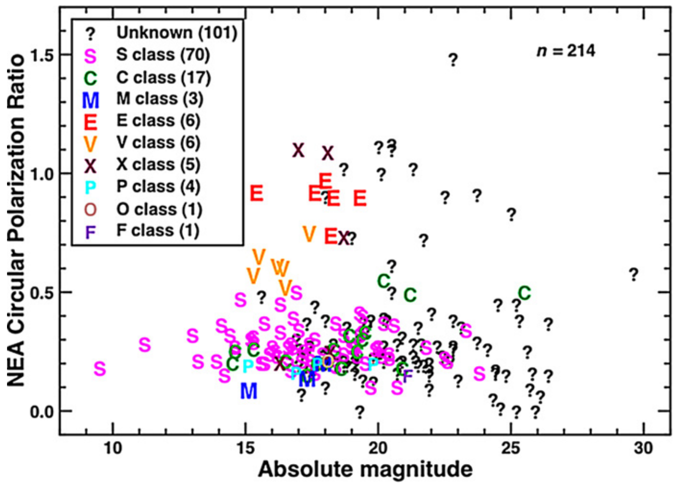

Fig. 1. Distribution of NEA SC/OC versus absolute magnitude. Spectral classes are indicated with different letters and colors. We adopt the classes described in Tholen and Barucci (1989), which identifies 14 groups based on the shape of their visible spectra and their albedos. S, Q, K, and L subclasses within the taxonomy in Bus et al. (2002) have been grouped into the S class. Dark C and B objects are labeled as "C." Of the 214 objects in the radar sample, estimates of VIS/IR spectral class are available for 113.

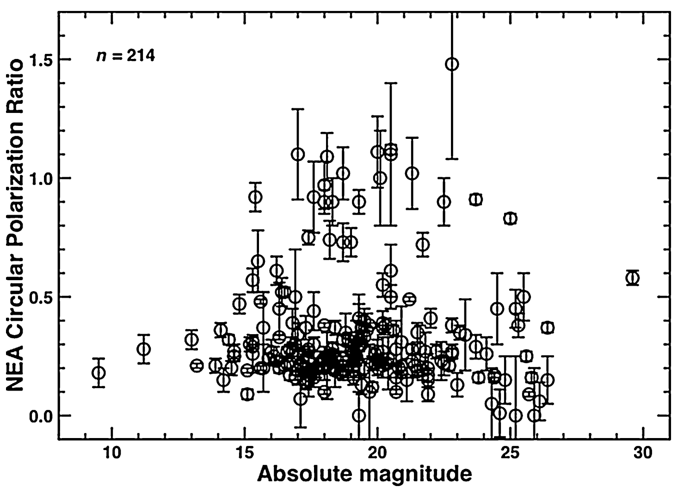

Fig. 2. Distribution of NEA SC/OC versus absolute magnitude including estimated standard errors on SC/OC. Standard errors are 1σ and are estimated using methods given in Ostro (2007). For objects observed on multiple dates, errors give the range of SC/OC.

and visible-infrared (VIS/IR) taxonomic class, as well as unexpected diversity in the decimeter-scale roughness of NEA surfaces.

NEA SC/OC estimates range from zero to 1.5, with a mean of 0.34 ± 0.25 and a median of 0.26, and 12% (26/214) have SC/OC exceeding 0.6, indicating that decimeter-scale surface roughness among NEAs is relatively common. Conversely, only ∼5% have SC/OC less than 0.1, indicating that smooth surfaces among the NEAs are uncommon. Of the objects in the radar sample, estimates of VIS/IR spectral class (Tholen and Barucci, 1989) are available for 113 (53%). The classes have been reported by several authors and are here converted to the Tholen and Barucci (1989) system.

All twelve classified objects with SC/OC exceeding 0.6 are in the E, V, or X classes (Table 2). The V class is associated with the howardite, eucrite, and diogenite basaltic achondrite meteorites, which originated either from mainbelt Asteroid 4 Vesta (Consolmagno and Drake, 1977) or from several NEAs thought to be cratering ejecta from it (Cruikshank et al., 1991). Most basaltic achondrites are breccias (Wasson, 1985). E class asteroids

Table 1
Summary of asteroid SC/OC distributions by spectral class.

Spectral class	Near-Earth SC/OC				Main-belt SC/OC			
	Mean	SD	Range	Number	Mean	SD	Range	Number
C	0.285	0.120	0.40	17	0.098	0.056	0.22	25
E	0.892	0.079	0.23	6	0.67	0.226	0.32	2
F	0.15	–	–	1	0.058	0.101	0.26	6
G					0.102	0.080	0.20	5
M	0.143	0.055	0.11	3	0.153	0.097	0.23	6
O	0.21	–	–	1				
PD	0.188	0.019	0.04	4	0.096	0.062	0.18	9
S	0.270	0.079	0.40	70	0.198	0.094	0.35	27
V	0.603	0.088	0.23	6	0.28	–	–	1
X	0.674	0.436	0.90	5				
?	0.339	0.284	1.48	101				

Notes. Main-belt asteroid results are from Magri et al. (2007a) except for the two E-class MBAs, which are from Shepard et al. (2008b). "?" indicates objects with unknown taxonomies. "X" refers to the degenerate E, M, and P objects (Tholen and Barucci, 1989; Bus et al., 2002). Table 2 lists SC/OC estimates in decreasing order and Table 3 lists SC/OC for objects ordered by catalog number and provisional designation. A histogram for the NEAs appears in Fig. 3. NEA SC/OC estimates range from zero to 1.5, with a mean of 0.34 ± 0.25 and a median of 0.26.

are associated with the enstatite achondrites (Zellner et al., 1977; Gaffey et al., 1992; Clark et al., 2004), also known as aubrites, whose composition is predominantly the orthopyroxene enstatite ($MgSiO_3$). Aubrites contain white enstatite crystals up to ten centimeters in diameter and small amounts of olivine, plagioclase, clinopyroxene, sulfides, and nickel–iron metal (Zellner et al., 1977; Clark et al., 2004), which suggests that they cooled underground under highly reducing conditions (McSween, 1999). Most aubrites consist of angular pieces or fragments in a softer matrix (Sears, 1995) and some are fragile (Hutchison, 2006).

The bulk of classified targets in the tables are C or S, which include carbonaceous and ordinary chondrite analogues (Burbine et al., 2002; Lipschutz and Schultz, 2007), respectively, as well as stony-iron analogues. Chondrites are undifferentiated, constitute the vast majority (∼80%) of meteorite falls, and are derived from asteroids that never melted (Lipschutz and Schultz, 2007). Our C and S targets have SC/OC from ∼0.1 to ∼0.5. The lowest SC/OC targets include our sample's handful of objects in the M spectral class (SC/OC from 0.1 to 0.2), which includes iron meteorite and enstatite–chondrite analogues (Burbine et al., 2002; Rivkin et al., 2002), and four members of the P class, which are thought to be dark, primitive, carbonaceous objects from the outer main belt (Bell et al., 1989). The X group is a degenerate class comprised of E, M, and P objects that have nearly indistinguishable VIS/IR spectra and which can be separated primarily by their optical albedos (Tholen and Barucci, 1989). Our five X objects include two with SC/OC = 1.1, one with SC/OC = 0.7, and two with SC/OC ∼ 0.2.

How can the striking correlation of SC/OC with spectral class be understood? One possibility is that mineralogy has played a major role in determining the centimeter-to-decimeter structural complexity of NEA surfaces, perhaps to the point that mineralogy is entirely responsible for the correlation in Fig. 1. Structural complexity in that scale regime is much more common on E and V NEAs than on chondritic or M-class NEAs. The smoothness of the metallic M-class NEAs [1986 DA (Ostro et al., 1991a) and perhaps 1950 DA (Busch et al., 2007)] may be due to the superior strength of metal; the average stony meteorite compressive strength is 200 MPa while the average iron meteorite compressive strength is 430 MPa (Petrovic, 2001). Such strength may have resulted in less ejecta in that size range being produced, which could suppress SC/OC produced by multiple scattering from fragments embedded in a fine-grained matrix. The roughness of the E and V NEAs may reflect integrity of their constituent mineralog-

Please cite this article in press as: Benner, L.A.M., et al. Near-Earth asteroid surface roughness depends on compositional class. Icarus (2008), doi:10.1016/j.icarus.2008.06.010

Table 2
Ranked list of near-Earth asteroid circular polarization ratios.

	Object	*H*	Class	SC/OC	Obs	Year	References
	2003 TH2	22.8		1.48 ± 0.4	A	2003	
	2005 WC1	20.6		1.12 ± 0.02	G	2005	
	2003 GY	20.0		1.11 ± 0.15	A	2003	
17511	1992 QN	16.9	X	1.10 ± 0.19	G	1996	Benner et al. (1997)
	2000 EE104	20.1		1.1 ± 0.3	A	2000	Howell et al. (2001)
141593	2002 HK12	18.1	X	1.09 ± 0.06	A	2002	
2101	Adonis	18.7		1.02 ± 0.11	A	1984	Benner et al. (1997)
	2005 TU50	21.3		1.02 ± 0.15	A	2005	
	2002 VE68	20.3		1.0 ± 0.2	G	2002	
33342	1998 WT24	17.9	E	0.97 ± 0.10	G A	2001	Busch et al. (2008)
3103	Eger	15.4	E	0.92 ± 0.06	A G	1986, 1991, 1996	Benner et al. (1997)
	2005 WJ56	17.6	E	0.92 ± 0.15	A G	2008	
	2001 CP36	23.7		0.91 ± 0.02	A	2001	
152770	1999 RR28	18.3	E	0.9 ± 0.1	A G	2005	
	2004 DC	18.0		0.9 ± 0.05	A G	2006	Taylor et al. (2006)
	2004 XP14	19.5	E	0.9 ± 0.05	G	2006	Benner et al. (2006b)
	2005 WK56	22.5		0.90 ± 0.10	A	2005	
	2001 WM15	25.0		0.83 ± 0.02	A	2001	
3908	Nyx	17.4	V	0.75 ± 0.03	A G	1988	Benner et al. (2002a)
4660	Nereus	18.2	E	0.74 ± 0.08	A	2002	Brozovic et al. (2008)
87024	2000 JS66	18.6	X	0.73 ± 0.08	A	2004	
	2005 TF49	19.0		0.73 ± 0.06	A	2006	
	2003 SS84	21.8		0.72 ± 0.05	G	2003	
1981	Midas	15.5	V	0.65 ± 0.13	A G	1987	Ostro et al. (1991b)
164121	2003 YT1	16.2	V	0.61 ± 0.06	A	2004	
	2001 YE4	20.5		0.61 ± 0.11	A	2002	
	2006 RH120	29.6		0.58 ± 0.03	G	2007	
7889	1994 LX	15.3	V	0.57 ± 0.05	A	2005	
	2006 RZ	20.3	C	0.55 ± 0.05	G	2006	
5381	Sekhmet	16.5	V	0.52 ± 0.02	A	2003	
5604	1992 FE	16.4	V	0.52 ± 0.06	G A	2002	
1566	Icarus	16.9	S	0.5 ± 0.2	G	1996	Mahapatra et al. (1999)
	1998 KY26	25.5	C	0.5 ± 0.1	G	1998	Ostro et al. (1999a)
	2002 KK8	20.5		0.50 ± 0.05	A	2002	
	2004 XL14	21.2	C	0.49 ± 0.01	G	2006	
4486	Mithra	15.6		0.48 ± 0.01	G	2000	
3199	Nefertiti	14.8	S	0.47 ± 0.04	A	1986	Shepard et al. (2004)
66391	1999 KW4 α	16.5	S	0.45 ± 0.11	G A	2001	Ostro et al. (2006)
	β			0.45 ± 0.20	G A	2001	Ostro et al. (2006)
	2004 AD	24.5		0.45 ± 0.15	A	2004	
	2005 FA	25.2		0.45 ± 0.08	A	2005	
	2002 SY50	17.6		0.44 ± 0.08	G	2002	
	2002 TD60	19.2	S	0.41 ± 0.10	A	2002	
	2003 HN16	22.0		0.41 ± 0.04	A	2003	
	2007 DT103	19.2	S	0.40 ± 0.05	G	2007	
2062	Aten	16.8	S	0.39 ± 0.06	G	1995	Benner et al. (1997)
89136	2001 US16	20.2		0.39 ± 0.05	G	2004	
	2000 UK11	25.0		0.38 ± 0.05	G	2000	
	2005 JE46	17.8		0.38 ± 0.01	G	2005	
	2005 OE3	20.3		0.38 ± 0.03	G	2005	
	2006 WB	22.8		0.38 ± 0.03	A	2006	
	2007 XH16	19.7		0.38 ± 0.01	A	2007	
5189	1990 UQ	17.3		0.37 ± 0.05	G	1992	
5660	1974 MA	15.7	S	0.37 ± 0.15	A	2005	
11500	1989 UR	18.4	S	0.37 ± 0.03	G	2007	
	2003 QB30	26.4		0.37 ± 0.02	A	2003	
	2004 VW14	19.4		0.37 ± 0.05	A	2008	
	2007 TU24	20.2	S	0.37 ± 0.01	G	2008	
4953	1990 MU	14.1	S	0.36 ± 0.03	G	1994	
38071	1999 GU3	19.4		0.36 ± 0.07	G	1999	Pravec et al. (2000b)
	2005 ED318	20.7	S	0.36 ± 0.02	G	2005	
	1998 BY7	21.4		0.35 ± 0.04	G	1998	
	1999 NW2	23.1		0.35 ± 0.03	G	1999	
	2002 FC	18.8		0.35 ± 0.08	G	2002	
10115	1992 SK	17.0	S	0.34 ± 0.05	G	1999	Busch et al. (2006)
	1999 TY2	23.3	S	0.34 ± 0.15	A	1999	
1862	Apollo	16.3	S	0.33 ± 0.01	A	1980	Ostro et al. (1991b)
	2002 NY40	19.2	S	0.33 ± 0.07	A	2002	
	2006 BQ6	19.7	C	0.33 ± 0.03	G	2006	
1866	Sisyphus	13.0	S	0.32 ± 0.04	A	1985	Ostro et al. (1991b)
4183	Cuno	14.4	S	0.32 ± 0.02	A	2000	
6037	1988 EG	18.7	S	0.32 ± 0.02	G	1998	
138258	2000 GD2	19.1	S	0.32 ± 0.15	G	2002	
	2005 CR37	18.9	C?	0.32 ± 0.03	A	2005	Benner et al. (2006a)

(*continued on next page*)

Please cite this article in press as: Benner, L.A.M., et al. Near-Earth asteroid surface roughness depends on compositional class. Icarus (2008), doi:10.1016/j.icarus.2008.06.010

Table 2 (*continued*)

	Object	*H*	Class	SC/OC	Obs	Year	References
2201	Oljato	15.3	S	0.31 ± 0.02	A	1983	Ostro et al. (1991b)
	2004 RQ10	20.9		0.31 ± 0.15	A	2004	
4769	Castalia	16.9		0.30 ± 0.02	A G	1989	Ostro et al. (1991b)
11066	Sigurd	15.2	S	0.30 ± 0.03	A	2004	
52760	1998 ML14	17.6	S	0.30 ± 0.03	G A	1998	Ostro et al. (2001)
	1998 ST27	19.5	C	0.30 ± 0.01	A	2001	Benner et al. (2003)
	2003 TL4	19.4		0.30 ± 0.03	G	2003	
4179	Toutatis	15.3	S	0.29 ± 0.01	G	1996	Ostro et al. (1999b)
	2003 EP4	23.7		0.29 ± 0.04	A	2003	
433	Eros	11.2	S	0.28 ± 0.06	G A	1988	Magri et al. (2001)
7025	1993 QA	18.0		0.28 ± 0.03	G	1996	
7822	1991 CS	17.4	S	0.28 ± 0.01	G	1996	Benner et al. (1999b)
22771	1999 CU3	16.7	S	0.28 ± 0.02	A	2003	
	2000 ED14	20.7		0.28 ± 0.12	A	2000	
	2003 MS2	21.0		0.28 ± 0.02	G	2003	
	2005 WA1	21.6		0.28 ± 0.10	A	2005	
1915	Quetzalcoatl	19.0	S	0.27 ± 0.08	A	1981	Shepard et al. (2004)
3757	1982 XB	19.0	S	0.27 ± 0.05	A	1987	Shepard et al. (2004)
7482	1994 PC1	16.8	S	0.27 ± 0.04	G	1997	
12711	1991 BB	16.0	S	0.27 ± 0.05	A	2000	
25143	Itokawa	19.0	S	0.27 ± 0.04	A	2001	Ostro et al. (2004)
30825	1990 TG1	14.6	S	0.27 ± 0.03	A	2005	
52387	1993 OM7	17.4		0.27 ± 0.02	A	2003	
152560	1991 BN	19.0	S	0.27 ± 0.04	A	2002	
	2001 BF10	22.3		0.27 ± 0.03	A	2001	
	2001 GQ2	20.0		0.27 ± 0.06	A	2001	
	2002 FD6	22.2		0.27 ± 0.03	G	2002	
	2006 VV2	16.8	S	0.27 ± 0.02	A	2007	
	2007 VD12	20.0	S	0.27 ± 0.05	G	2007	
14827	Hypnos	18.2	C?	0.26 ± 0.02	G	1986	Ostro et al. (1989)
163732	2003 KP2	15.3	C	0.26 ± 0.08	A	2003	
179806	2002 TD66	19.9	S	0.26 ± 0.02	A	2008	
	2001 SE286	17.1		0.26 ± 0.01	A	2001	
	2002 AA29	24.1		0.26 ± 0.07	A	2003	Ostro et al. (2003)
	2005 EU2	23.1		0.26 ± 0.02	A G	2005	
2100	Ra-Shalom	16.1	S	0.25 ± 0.04	A	1984, 2000, 2003	Shepard et al. (2000, 2008a)
3200	Phaethon	14.6	B	0.25 ± 0.02	A	2007	
4197	1982 TA	14.6	S	0.25 ± 0.02	G	1996	
22753	1998 WT	17.4	S	0.25 ± 0.03	G	2005	
85774	1998 UT18	19.1	C	0.25 ± 0.01	A	2003	
144900	2004 VG64	18.2	S	0.25 ± 0.02	A	2005	
162181	1999 LF6	18.2		0.25 ± 0.01	A	2004	
185851	2000 DP107	18.0	M	0.25 ± 0.02	G	2000	
	2003 RU11	25.6		0.25 ± 0.02	A	2003	
9856	1991 EE	17.4		0.24 ± 0.02	G	1991	
23187	2000 PN9	15.9	S	0.24 ± 0.02	A	2001	
26663	2000 XK47	18.0		0.24 ± 0.02	A	2001	
66063	1998 RO1	18.0	S	0.24 ± 0.05	A	2003	
	1994 XD	19.1		0.24 ± 0.05	A	2005	
	2000 CE59	20.2	S	0.24 ± 0.02	A	2000	
4450	Pan	17.2	S	0.23 ± 0.03	A	2008	
6239	Minos	17.9		0.23 ± 0.04	G	2004	
6489	Golevka	19.2	S	0.23 ± 0.02	G	1995	Hudson et al. (2000)
68950	2002 QF15	16.2	S	0.23 ± 0.02	A	2003	
162000	1990 OS	19.3		0.23 ± 0.03	A	1990	Ostro et al. (1991a, 1991b)
162416	2000 EH26	21.3		0.23 ± 0.07	A	2000	
	2000 YF29	20.2	S	0.23 ± 0.01	A	2001	
	2001 EB18	19.1		0.23 ± 0.05	A	2002	
	2001 EC16	22.2		0.23 ± 0.08	G	2001	
	2006 AM4	21.8	S	0.23 ± 0.02	A	2007	
68346	2001 KZ66	16.5	S	0.22 ± 0.02	A	2003	
85182	1991 AQ	17.1		0.22 ± 0.03	A	1991	
136770	1996 PC1	20.3		0.22 ± 0.02	A	2001	
	1999 FN19	22.4	S	0.22 ± 0.05	G	1999	
	2000 QW7	19.4		0.22 ± 0.03	G	2000	
	2000 UG11	20.3	S	0.22 ± 0.11	G	2000	
1627	Ivar	13.2	S	0.21 ± 0.01	A	1985	Ostro et al. (1990)
1917	Cuyo	13.9	S	0.21 ± 0.03	A G	1989	Ostro et al. (1991a, 1991b)
2063	Bacchus	17.1	S	0.21 ± 0.01	G	1996	Benner et al. (1999a)
4034	1986 PA	18.1	O	0.21 ± 0.14	A	1989	Shepard et al. (2004)
54509	YORP	22.6	S	0.21 ± 0.02	G A	2001	Taylor et al. (2007)
	2005 NB7	18.7	S	0.21 ± 0.01	A	2008	
	1999 MN	21.4		0.21 ± 0.05	A	2005	
	2000 RD53	19.9		0.21 ± 0.05	G	2000	

(*continued on next page*)

Please cite this article in press as: Benner, L.A.M., et al. Near-Earth asteroid surface roughness depends on compositional class. Icarus (2008), doi:10.1016/j.icarus.2008.06.010

Table 2 (*continued*)

	Object	*H*	Class	SC/OC	Obs	Year	References
	2002 AY1	20.6		0.21 ± 0.02	A	2002	
	2002 CE26	16.8	C	0.21 ± 0.02	A	2004	Shepard et al. (2006)
	2003 UC20	18.1	C	0.21 ± 0.03	A	2003	
	2006 GY2	18.7		0.21 ± 0.02	G	2006	
1620	Geographos	15.6	S	0.20 ± 0.01	A G	1983, 1994	Ostro et al. (1996)
1580	Betulia	14.5	C	0.20 ± 0.03	A G	2002	Magri et al. (2007b)
16834	1997 WU22	15.4	S	0.20 ± 0.10	A	2000	
35396	1997 XF11	16.9	X	0.20 ± 0.02	G	2002	
37655	Illapa	17.7	C	0.20 ± 0.04	G	2003	
65803	Didymos	18.0	M	0.20 ± 0.02	G	2003	
100085	1992 UY4	17.6	P	0.20 ± 0.02	G A	2005	
138971	2001 CB21	18.4		0.20 ± 0.02	A	2006	
163692	2003 CY18	18.0		0.20 ± 0.05	A	2005	
164211	2004 JA27	19.3	S	0.20 ± 0.04	A	2004	
	2002 AL14	17.7	S	0.20 ± 0.01	A	2002	
	2002 BG25	20.8		0.20 ± 0.02	A	2002	
	2002 BM26	20.0	P	0.20 ± 0.03	A	2002	
	2006 UQ17	21.9		0.20 ± 0.06	A	2007	
7335	1989 JA	17.0		0.19 ± 0.06	A G	1989	Mahapatra et al. (2002)
8014	1990 MF	18.7		0.19 ± 0.04	A	1990	Ostro et al. (1991b)
53319	1999 JM8	15.0	P	0.19 ± 0.01	G A	1999	Benner et al. (2002b)
69230	Hermes	17.5	S	0.19 ± 0.02	G	2003	
85938	1999 DJ4	18.5	S	0.19 ± 0.02	A	2004	
162039	1996 JG	19.1		0.19 ± 0.04	G	1996	
	1999 FN53	18.4		0.19 ± 0.07	G	1999	
	2000 LF3	21.6		0.19 ± 0.02	A	2000	
	2001 BE10	19.1		0.19 ± 0.02	A	2004	
	2003 HM	21.7		0.19 ± 0.04	A	2003	
1036	Ganymed	09.5	S	0.18 ± 0.06	A	1985	Ostro et al. (1991b)
101955	1999 RQ36	20.8	C	0.18 ± 0.01	G A	1999	
	2001 SG276	17.7		0.18 ± 0.03	A	2001	
7341	1991 VK	16.7	S	0.17 ± 0.02	A	2007	
7753	1988 XB	18.6	S	0.17 ± 0.02	A	2007	
144901	2004 WG1	17.4		0.17 ± 0.01	A	2006	
	2001 FR85	24.5		0.17 ± 0.01	A	2001	
	2001 YP3	21.9		0.17 ± 0.03	A	2002	
13651	1997 BR	17.6	S	0.16 ± 0.04	G	1997	
65909	1998 FH12	19.1		0.16 ± 0.03	G	2003	
153591	2001 SN263	16.9	P	0.16 ± 0.01	A	2008	
	2000 YA	23.7	S	0.16 ± 0.02	A	2000	
	2001 SP263	25.6		0.16 ± 0.02	A	2001	
	2002 TS69	24.5		0.16 ± 0.02	A	2002	
	2004 VB	20.8		0.16 ± 0.05	A	2004	
1685	Toro	14.2	S	0.15 ± 0.05	A	1980	Ostro et al. (1983)
	2000 EW70	21.1	F	0.15 ± 0.09	A	2000	
	2001 XX4	22.0		0.15 ± 0.03	A	2001	
	2005 AB	17.5	C	0.15 ± 0.04	A	2005	
	2005 EK70	17.4		0.15 ± 0.07	A	2008	
	2005 TD49	26.4		0.15 ± 0.10	A	2005	
	2007 FY20	24.8		0.15 ± 0.10	A	2007	
29075	1950 DA	16.8	M	0.14 ± 0.03	A G	2001	Busch et al. (2007)
	1989 AZ	19.4		0.13 ± 0.04	A	2008	
	2004 HX53	23.3		0.13 ± 0.05	A	2004	
141432	2002 CQ11	19.9		0.12 ± 0.02	A	2003	
99942	Apophis	19.7	S	0.1 ± 0.2	A	2005, 2006	Giorgini et al. (2008)
	2002 AV	20.7	S	0.10 ± 0.01	A	2002	
	2004 RF84	18.2		0.10 ± 0.01	A	2005	
6178	1986 DA	15.1	M	0.09 ± 0.02	A	1986	Ostro et al. (1991b)
	2001 UP	25.7		0.09 ± 0.01	A	2001	
	2004 FY31	21.9		0.09 ± 0.03	A	2004	
4544	Xanthus	17.1		0.07 ± 0.12	A	1990	Benner et al. (1997)
	2005 XA	26.1		0.06 ± 0.08	A	2005	
	2005 HB4	24.3		0.05 ± 0.15	A	2005	
	2001 AV43	24.4		0.01 ± 0.10	A	2001	
163295	2002 HW	19.3		0.0 ± 0.1	A	2005	
	2002 TZ66	25.9		0.0 ± 0.2	A	2002	
	2006 QV89	25.2		0.0 ± 0.25	A	2006	

Notes. "Object" gives the number, name, and/or provisional designation of the asteroid. "*H*" is the absolute magnitude. "Type" is the taxonomic class; if left blank, the class is unknown. "SC/OC" is the circular polarization ratio. Uncertainties are standard errors for objects observed on a single date and ranges of SC/OC for objects observed on multiple dates. "Obs" gives the observatory used, in chronological order: "A" is Arecibo and "G" is Goldstone. If both are given then the average from the observatories was used. "Year" indicates when the observations were obtained. Objects with "?" next to them are known to be optically dark based on their absolute magnitudes and radar-derived diameters and have been grouped in the C-class. "References" refer to previously published circular polarization ratios; for fields left blank, results are reported here for the first time. For 1999 KW4, we provide separate estimates for the primary (α) and secondary (β).

Please cite this article in press as: Benner, L.A.M., et al. Near-Earth asteroid surface roughness depends on compositional class. Icarus (2008), doi:10.1016/j.icarus.2008.06.010

Table 3
Ordered list of near-Earth asteroid circular polarization ratios.

Asteroid	*H* (mag)	Spectral class	SC/OC	Taxonomic reference
433 Eros	11.2	S	0.28 ± 0.06	Binzel et al. (2004)
1036 Ganymed	09.5	S	0.18 ± 0.06	Binzel et al. (2004)
1566 Icarus	16.9	S	0.5 ± 0.2	Tholen (1989), Hicks et al. (1998)
1580 Betulia	14.5	C	0.20 ± 0.03	Rivkin et al. (2005), Tholen (1989)
1620 Geographos	15.6	S	0.20 ± 0.01	Binzel et al. (2004)
1627 Ivar	13.2	S	0.21 ± 0.01	Binzel et al. (2004), Davies et al. (2007)
1685 Toro	14.2	S	0.15 ± 0.05	Binzel et al. (2004)
1862 Apollo	16.3	S	0.33 ± 0.01	Binzel et al. (2004)
1866 Sisyphus	13.0	S	0.32 ± 0.04	Binzel et al. (2004)
1915 Quetzalcoatl	19.0	S	0.27 ± 0.08	Tholen (1989)
1917 Cuyo	13.9	S	0.21 ± 0.03	Binzel et al. (2004)
1981 Midas	15.5	V	0.65 ± 0.13	Binzel et al. (2004)
2062 Aten	16.8	S	0.39 ± 0.06	Binzel et al. (2004)
2063 Bacchus	17.1	S	0.21 ± 0.01	Binzel et al. (2004)
2100 Ra-Shalom	16.1	S	0.25 ± 0.04	Shepard et al. (2008a)
2101 Adonis	18.7		1.02 ± 0.11	
2201 Oljato	15.3	S	0.31 ± 0.02	Binzel et al. (2004)
3103 Eger	15.4	E	0.92 ± 0.06	Binzel et al. (2004)
3199 Nefertiti	14.8	S	0.47 ± 0.04	Binzel et al. (2004)
3200 Phaethon	14.6	B	0.25 ± 0.02	Binzel et al. (2004)
3757 1982 XB	19.0	S	0.27 ± 0.05	Tholen (1989)
3908 Nyx	17.4	V	0.75 ± 0.03	Binzel et al. (2004)
4034 1986 PA	18.1	O	0.21 ± 0.14	Binzel et al. (2004)
4179 Toutatis	15.3	S	0.29 ± 0.01	Binzel et al. (2004), Davies et al. (2007)
4183 Cuno	14.4	S	0.32 ± 0.02	Binzel et al. (2004)
4197 1982 TA	14.6	S	0.25 ± 0.02	Binzel et al. (2004)
4450 Pan	17.2	S	0.23 ± 0.03	M.D. Hicks (pers. comm.)
4486 Mithra	15.6		0.48 ± 0.01	
4544 Xanthus	17.1		0.07 ± 0.12	
4660 Nereus	18.2	E	0.74 ± 0.08	Binzel et al. (2004), Delbo et al. (2003)
4769 Castalia	16.9		0.30 ± 0.02	
4953 1990 MU	14.1	S	0.36 ± 0.03	Hicks et al. (1998)
5189 1990 UQ	17.3		0.37 ± 0.05	
5381 Sekhmet	16.5	V	0.52 ± 0.02	Davies et al. (2007)
5604 1992 FE	16.4	V	0.52 ± 0.05	Binzel et al. (2004)
5660 1974 MA	15.7	S	0.37 ± 0.15	Binzel et al. (2004)
6037 1988 EG	18.7	S	0.32 ± 0.02	Fevig and Fink (2007)
6178 1986 DA	15.1	M	0.09 ± 0.02	Ostro et al. (1991a)
6239 Minos	17.9		0.23 ± 0.04	
6489 Golevka	19.2	S	0.23 ± 0.02	Binzel et al. (2004), Davies et al. (2007)
7025 1993 QA	18.0		0.28 ± 0.03	
7335 1989 JA	17.0		0.19 ± 0.06	
7341 1991 VK	16.7	S	0.17 ± 0.02	Binzel et al. (2004)
7482 1994 PC1	16.8	S	0.27 ± 0.04	Binzel et al. (2004)
7753 1988 XB	18.6	C	0.18 ± 0.02	Binzel et al. (2004)
7822 1991 CS	17.4	S	0.28 ± 0.01	Binzel et al. (2004)
7889 1994 LX	15.3	V	0.57 ± 0.05	Binzel et al. (2004)
8014 1990 MF	18.7		0.19 ± 0.04	
9856 1991 EE	17.4	S	0.24 ± 0.02	Harris et al. (1998)
10115 1992 SK	17.0	S	0.34 ± 0.05	Binzel et al. (2004)
11066 Sigurd	15.2	S	0.30 ± 0.03	Binzel et al. (2004)
11500 1989 UR	18.4	S	0.37 ± 0.03	Binzel et al. (2004)
12711 1991 BB	15.7	S	0.27 ± 0.05	Binzel et al. (2004)
13651 1997 BR	17.6	S	0.16 ± 0.04	Binzel et al. (2004)
14827 Hypnos	18.2	C?	0.26 ± 0.02	Ostro et al. (1989)
16834 1997 WU22	15.4	S	0.20 ± 0.10	Binzel et al. (2004)
17511 1992 QN	16.9	X	1.10 ± 0.19	Binzel et al. (2004)
22753 1998 WT	17.4	S	0.25 ± 0.03	Whiteley (2001), Lazzarin et al. (2005)
22771 1999 CU3	16.7	S	0.28 ± 0.02	Binzel et al. (2004)
23187 2000 PN9	15.9	S	0.24 ± 0.02	I.N. Belskaya (pers. comm.)
25143 Itokawa	19.0	S	0.27 ± 0.04	Binzel et al. (2004), Davies et al. (2007)
26663 2000 XK47	18.0		0.24 ± 0.02	
29075 1950 DA	16.8	M	0.14 ± 0.03	Rivkin et al. (2005)
30825 1990 TG1	14.7	S	0.27 ± 0.03	F. De Meo, R.P. Binzel (pers. comm.)
33342 1998 WT24	17.9	E	0.97 ± 0.10	Lazzarin et al. (2004)
35396 1997 XF11	16.9	X	0.20 ± 0.02	Binzel et al. (2004)
37655 Illapa	17.7	C	0.20 ± 0.04	M.D. Hicks (pers. comm.)
38071 1999 GU3	19.4		0.36 ± 0.07	
52387 1993 OM7	17.4		0.27 ± 0.02	
52760 1998 ML14	17.6	S	0.30 ± 0.03	Davies et al. (2007)
53319 1999 JM8	15.0	P	0.19 ± 0.01	Binzel et al. (2004)
54509 YORP	22.6	S	0.21 ± 0.02	Gietzen and Lacy (2007)
65803 Didymos	18.0	M	0.20 ± 0.02	Binzel et al. (2004), Kitazato et al. (2004), Pravec et al. (2006)
65909 1998 FH12	19.1		0.16 ± 0.03	
66063 1998 RO1	18.0	S	0.24 ± 0.05	Abell et al. (2005)

(*continued on next page*)

Please cite this article in press as: Benner, L.A.M., et al. Near-Earth asteroid surface roughness depends on compositional class. Icarus (2008), doi:10.1016/j.icarus.2008.06.010

Table 3 (*continued*)

Asteroid		*H* (mag)	Spectral class	SC/OC	Taxonomic reference
66391	1999 KW4 α	16.5	S	0.45 ± 0.11	Binzel et al. (2004), Davies et al. (2007)
	β			0.45 ± 0.20	
68346	2001 KZ66	16.5	S	0.22 ± 0.02	Lazzarin et al. (2005)
68950	2002 QF15	16.2	S	0.23 ± 0.02	Abell et al. (2006), F. De Meo, R.P. Binzel (pers. comm.)
69230	Hermes	17.5	S	0.19 ± 0.02	Rivkin et al. (2004)
85182	1991 AQ	17.1		0.22 ± 0.03	
85774	1998 UT18	19.1	C	0.25 ± 0.01	Binzel et al. (2004)
85938	1999 DJ4	18.5	S	0.19 ± 0.02	Binzel et al. (2004)
87024	2000 JS66	18.6	X	0.73 ± 0.08	Lazzarin et al. (2005)
89136	2001 US16	20.2		0.39 ± 0.05	
99942	Apophis	19.7	S	0.1 ± 0.2	Binzel et al. (2006, 2007)
100085	1992 UY4	17.6	P	0.20 ± 0.02	Volquardsen et al. (2007)
101955	1999 RQ36	20.8	C	0.18 ± 0.01	Delbo et al. (2003)
136770	1996 PC1	20.3		0.22 ± 0.02	
138175	2000 EE104	20.1		1.1 ± 0.3	
138258	2000 GD2	19.1	S	0.32 ± 0.15	Binzel et al. (2004)
138971	2001 CB21	18.4		0.20 ± 0.02	
141432	2002 CQ11	19.9		0.12 ± 0.02	
141593	2002 HK12	18.1	X	1.09 ± 0.06	E.S. Howell (pers. comm.)
144900	2004 VG64	18.2	S	0.25 ± 0.02	F. De Meo, R.P. Binzel (pers. comm.)
144901	2004 WG1	17.4		0.17 ± 0.01	
152560	1991 BN	19.0	S	0.27 ± 0.04	Binzel et al. (2004)
152770	1999 RR28	18.3	E	0.9 ± 0.1	E.S. Howell (pers. comm.)
153591	2001 SN263	16.9	P	0.16 ± 0.01	R.P. Binzel (pers. comm.)
154276	2002 SY50	17.6		0.44 ± 0.08	
162000	1990 OS	19.3		0.23 ± 0.03	
162039	1996 JG	19.1		0.19 ± 0.04	
162181	1999 LF6	18.2		0.25 ± 0.01	
162416	2000 EH26	21.3		0.23 ± 0.07	
163295	2002 HW	19.3		0.0 ± 0.1	
163692	2003 CY18	18.0		0.20 ± 0.05	
163732	2003 KP2	15.3	C	0.26 ± 0.08	F. De Meo, R.P. Binzel (pers. comm.)
164121	2003 YT1	16.2	V	0.61 ± 0.06	Abell et al. (2005)
164211	2004 JA27	19.3	S	0.20 ± 0.04	F. De Meo, R.P. Binzel (pers. comm.)
179806	2002 TD66	19.9	S	0.26 ± 0.02	M.D. Hicks (pers. comm.)
185851	2000 DP107	18.0	M	0.25 ± 0.02	Pravec et al. (2006), Yang et al. (2003)
	1989 AZ	19.4		0.13 ± 0.04	
	1994 XD	19.1		0.21 ± 0.05	
	1998 BY7	21.4		0.35 ± 0.04	
	1998 KY26	25.5	C	0.5 ± 0.1	Ostro et al. (1999a)
	1998 ST27	19.5	C	0.30 ± 0.01	Abell et al. (2005)
	1999 FN19	22.4	S	0.22 ± 0.05	Binzel et al. (2004)
	1999 FN53	18.4		0.19 ± 0.07	
	1999 MN	21.4		0.21 ± 0.05	
	1999 NW2	23.1		0.35 ± 0.03	
	1999 TY2	23.3	S	0.34 ± 0.15	Pravec et al. (2000a)
	2000 CE59	20.2	S	0.24 ± 0.02	Binzel et al. (2004)
	2000 ED14	20.7		0.28 ± 0.12	
	2000 EW70	20.7	F	0.15 ± 0.09	Whiteley (2001)
	2000 LF3	21.6		0.19 ± 0.02	
	2000 QW7	19.4		0.22 ± 0.03	
	2000 RD53	19.9		0.21 ± 0.05	
	2000 UG11	20.3	S	0.22 ± 0.11	Kitazato et al. (2004)
	2000 UK11	25.0		0.38 ± 0.05	
	2000 YA	23.7	S	0.16 ± 0.02	Binzel et al. (2004)
	2000 YF29	20.2	S	0.23 ± 0.01	Binzel et al. (2004)
	2001 AV43	24.4		0.01 ± 0.10	
	2001 BE10	19.1		0.19 ± 0.02	
	2001 BF10	22.3		0.27 ± 0.03	
	2001 CP36	23.7		0.91 ± 0.02	
	2001 EB18	19.1		0.23 ± 0.05	
	2001 EC16	22.2		0.23 ± 0.08	
	2001 FR85	24.5		0.17 ± 0.01	
	2001 GQ2	20.0		0.27 ± 0.06	
	2001 SE286	17.1		0.26 ± 0.01	
	2001 SG276	17.7		0.18 ± 0.03	
	2001 SP263	25.6		0.16 ± 0.02	
	2001 UP	25.7		0.09 ± 0.01	
	2001 WM15	25.0		0.83 ± 0.02	
	2001 XX4	22.0		0.15 ± 0.03	
	2001 YE4	20.5		0.61 ± 0.11	
	2001 YP3	21.9		0.17 ± 0.03	
	2002 AA29	24.1		0.26 ± 0.07	
	2002 AL14	17.7	S	0.20 ± 0.01	Binzel et al. (2004)
	2002 AV	20.7	S	0.10 ± 0.01	Binzel et al. (2004)
	2002 AY1	20.6		0.21 ± 0.02	

(*continued on next page*)

Please cite this article in press as: Benner, L.A.M., et al. Near-Earth asteroid surface roughness depends on compositional class. Icarus (2008), doi:10.1016/j.icarus.2008.06.010

Table 3 (*continued*)

Asteroid	*H* (mag)	Spectral class	SC/OC	Taxonomic reference
2002 BG25	20.8		0.20 ± 0.02	
2002 BM26	20.0	P	0.20 ± 0.03	Binzel et al. (2004), Delbo et al. (2003)
2002 CE26	16.8	C	0.21 ± 0.02	Shepard et al. (2006)
2002 FC	18.8		0.35 ± 0.08	
2002 FD6	22.2		0.27 ± 0.03	
2002 KK8	20.5		0.50 ± 0.05	
2002 NY40	19.2	S	0.33 ± 0.07	Rivkin et al. (2003)
2002 TD60	19.2	S	0.41 ± 0.10	Lazzarin et al. (2005)
2002 TS69	24.5		0.16 ± 0.02	
2002 TZ66	25.9		0.0 ± 0.2	
2002 VE68	20.3		1.0 ± 0.2	
2003 EP4	23.7		0.29 ± 0.04	
2003 GY	20.0		1.11 ± 0.15	
2003 HM	21.7		0.19 ± 0.04	
2003 HN16	22.0		0.41 ± 0.04	
2003 MS2	21.0		0.28 ± 0.02	
2003 QB30	26.4		0.37 ± 0.02	
2003 RU11	25.6		0.25 ± 0.02	
2003 SS84	21.8		0.72 ± 0.05	
2003 TH2	22.8		1.48 ± 0.4	
2003 TL4	19.4		0.30 ± 0.03	
2003 UC20	18.1	C	0.21 ± 0.03	Abe et al. (2007)
2004 AD	24.5		0.45 ± 0.15	
2004 DC	18.0		0.9 ± 0.05	
2004 FY31	21.9		0.09 ± 0.03	
2004 HX53	23.3		0.13 ± 0.05	
2004 RF84	18.2		0.10 ± 0.01	
2004 RQ10	20.9		0.31 ± 0.15	
2004 VB	20.8		0.16 ± 0.05	
2004 VW14	19.4		0.37 ± 0.05	
2004 XL14	21.2	C	0.49 ± 0.01	F. De Meo, R.P. Binzel (pers. comm.)
2004 XP14	19.5	E	0.9 ± 0.05	Reddy et al. (2006)
2005 AB	17.5	C	0.15 ± 0.04	Kumar et al. (2006)
2005 CR37	18.9	C?	0.32 ± 0.03	Benner et al. (2006a)
2005 ED318	20.7	S	0.36 ± 0.02	F. De Meo, R.P. Binzel (pers. comm.)
2005 EK70	17.4		0.15 ± 0.07	
2005 EU2	23.1		0.26 ± 0.02	
2005 FA	25.2		0.45 ± 0.08	
2005 HB4	24.3		0.05 ± 0.15	
2005 JE46	17.8		0.38 ± 0.01	
2005 NB7	18.7		0.24 ± 0.01	
2005 OE3	20.3		0.38 ± 0.03	
2005 TD49	26.4		0.15 ± 0.10	
2005 TF49	19.1		0.73 ± 0.06	
2005 TU50	21.3		1.02 ± 0.15	
2005 WA1	21.6		0.28 ± 0.10	
2005 WC1	20.6		1.12 ± 0.02	
2005 WJ56	17.6		0.92 ± 0.15	M.D. Hicks, (pers. comm.) V. Reddy (pers. comm.)
2005 WK56	22.5		0.90 ± 0.10	
2005 XA	26.1		0.06 ± 0.08	
2006 AM4	21.8	S	0.23 ± 0.02	M.D. Hicks (pers. comm.)
2006 BQ6	19.7	C	0.33 ± 0.03	M.D. Hicks (pers. comm.)
2006 GY2	18.7		0.21 ± 0.02	
2006 QV89	25.2		0.0 ± 0.25	
2006 RH120	29.6		0.58 ± 0.03	
2006 RZ	20.3	C	0.55 ± 0.05	F. De Meo, R.P. Binzel (pers. comm.)
2006 UQ17	21.9		0.20 ± 0.06	
2006 VV2	16.8	S	0.27 ± 0.02	V. Reddy (pers. comm.)
2006 WB	22.8		0.38 ± 0.03	
2007 DT103	19.2	S	0.40 ± 0.05	Hicks and Somers (2007)
2007 FY20	24.8		0.15 ± 0.10	
2007 TU24	20.2	S	0.37 ± 0.01	M.D. Hicks (pers. comm.)
2007 VD12	20.0	S	0.27 ± 0.05	M.D. Hicks (pers. comm.)
2007 XH16	19.7		0.38 ± 0.01	

Notes. Circular polarization ratios listed in order of asteroid number, and then in order of provisional designation for unnumbered objects. *H* is the absolute magnitude, which were obtained from the JPL/Horizons database (http://ssd.jpl.nasa.gov/?Horizons). Spectral class is indicated if known; if not, the field is left blank.

ical assemblages at those scales, perhaps due to the presence of large crystals (especially in aubrites and diogenites) formed during cooling and solidification of molten material in the parent bodies, and/or their predominantly brecciated textures (Wasson, 1985), and/or unique collisional histories of those bodies. Chondrites are nebular condensates that have been ground down by collisions and comminution into smaller fragments than the achondrites, perhaps explaining the intermediate polarization ratios of their candidate NEA analogues. The S class may also include an unknown number of stony-iron analogues that, because of their abundant metal, could have polarization signatures similar to those of metallic M types. Thus, some of the S-class NEAs with the smallest SC/OC may be objects mineralogically akin to stony-irons rather than to ordinary chondrites.

Please cite this article in press as: Benner, L.A.M., et al. Near-Earth asteroid surface roughness depends on compositional class. Icarus (2008), doi:10.1016/j.icarus.2008.06.010

It is also possible that the correlation in Fig. 1 primarily reflects differences in the formation ages and/or collisional histories of the objects in the different classes. The polarization ratio is sensitive to the abundance of near-surface dielectric interfaces with radii of curvature comparable to the wavelength. For NEA surfaces, there are many factors that determine this abundance. The presence of a thick regolith depleted in rocks by long-term micrometeorite gardening, such as exists in ancient regions on the Moon, generally lowers SC/OC (Campbell, 2002), but the trade-off between production of such material by impacts, depletion of it by impacts, and impact-induced migration of it from the interior (Miyamoto et al., 2007) is unknown and may be very different for different NEAs.

If we suppose that formation age rather than mineralogy is primarily responsible for the trend seen in Fig. 1, then it is equally plausible that E class NEAs' high polarization ratios are due to them being extremely young as they are due to them being relatively ancient. On the Moon, some areas with high SC/OC correlate strongly with macroscopically rugged, geologically young crater walls and ejecta and with near-grazing incidence angles (Campbell, 2002; Campbell and Campbell, 2006). However, the E class meteorite analogues, the aubrites, have the oldest average cosmic ray exposure ages among stony meteorites (McSween, 1999; Eugster et al., 2006), directly contradicting this simple hypothesis. Perhaps the E class NEAs have high SC/OC because their relatively old surfaces have accumulated low radar loss tangent regoliths on top of topographically rugged subsurfaces.

NEAs have higher polarization ratios than mainbelt asteroids (MBAs). A recent radar study of 82 MBAs (Magri et al., 2007a) revealed a mean circular polarization ratio of 0.14 ± 0.098 (Table 1), less than half the NEA value. S-class MBAs have higher circular polarization ratios than other MBAs, possibly due to different mineralogy (material strength or loss tangent), a different impactor population, or both. For our NEA sample, the S and C class means of 0.27 ± 0.079 and 0.29 ± 0.12 are indistinguishable and suggest similar near-surface structural complexity on average. However, within each group SC/OC varies by up to 0.40, implying much more structural diversity than for the MBA groups. Vesta, the only V-class MBA detected by radar, is a 530-km-diameter object with SC/OC $= 0.28 \pm 0.05$, larger than $\sim$90% of MBA circular polarization ratios (Magri et al., 2007a). Only the M-class NEAs have SC/OC comparable to those of MBAs in the same class, which could be due to the strength of metal (for M-objects that are actually metallic) and its effect on regolith generation, a small sample size, or some other factor.

The differences between the NEA and MBA SC/OC distributions indicate that the two populations have dramatically different surfaces. This is not surprising given that NEAs are younger, smaller, and have much weaker gravitational fields. Whereas MBA surfaces are dominated by mostly fine-grained regoliths that have matured during several billion years of impact bombardment, NEA surfaces retain only the low-velocity tail of the impact ejecta distribution, which is likely to involve a size partioning that favors large ejecta. Our results are consistent with the production of larger particles and their resistance to erosion from meteoroid bombardment being dependent on mineralogical composition.

The 25 binary NEAs observed by radar have a mean SC/OC $=$ 0.33 ± 0.19 and a median of 0.25 that are indistinguishable from the NEA population as a whole, and a range from 0.15 to 0.9. The average NEA circular polarization ratio is comparable to that of comet nuclei detected by radar (SC/OC $= 0.35 \pm 020$, Table 4), hinting at a similar degree (but not necessarily style) of surface complexity, but the comet sample size is only six and has a range less than half that of the NEA sample, so detailed comparisons must wait until more comets are observed.

Table 4
Comet nucleus circular polarization ratios.

Comet	SC/OC	Reference
2P/Encke	0.21 ± 0.04	Harmon and Nolan (2005)
26P/Grigg–Skjellerup	<0.3	Kamoun et al. (1999)
P/2005 JQ5 Catalina	0.49 ± 0.05	Harmon et al. (2006)
C/IRAS–Araki–Alcock	0.105 ± 0.005	Harmon et al. (1989)
C/Sugano–Saigusa–Fujikawa	0.23 ± 0.03	Harmon et al. (1999)
C/1996 B2 Hyakutake	0.49 ± 0.10	Harmon et al. (1997)
C/1998 K5 LINEAR	<0.5	Harmon et al. (1999)
C/2004 Q2 Machholz	0.59 ± 0.04	Nolan et al. (2005)

Notes. Comet circular polarization ratios from the references shown on the right. Excluding P/Grigg–Skjellerup and 1998 K5, which have only upper limits, the mean SC/OC for the other six comets is 0.35 ± 0.20.

The correspondence of centimeter to decimeter-scale surface (or near-surface) structure to VIS/IR spectral class supports association of classes with distinct mineralogies and meteorite types, and reveals distinct differences in the macroscale structural complexity of objects in different spectral classes. The two radar-detected NEAs visited by spacecraft, the S-class objects 433 Eros and 25143 Itokawa, have SC/OC $= 0.28 \pm 0.06$ (Magri et al., 2001) and 0.27 ± 0.04 (Ostro et al., 2004) that are indistinguishable from the NEA median; the structural complexity of their surfaces may be fairly representative of many S and C-class NEAs, but it is very much less severe than that on E and V-class NEAs. In spacecraft images at comparable scales, the surfaces appear to have different roughnesses, but to the radar they look very similar, perhaps implying different degrees of subsurface scattering and/or regolith thicknesses between the two objects. Given the trend we see here, the high SC/OC X-class objects in our sample will probably turn out to be E-class rather than M-class or P-class objects once optical albedos are available. In September 2008, the *Rosetta* spacecraft will encounter E-class MBA 2867 Steins (Barucci et al., 2005; Fornasier et al., 2006); given the results presented here, we expect that very high-resolution optical images would reveal a surface much more rugged at decimeter scales than those seen by spacecraft on any asteroid to date. Determination of the spectral types of the 101 unclassified NEAs in the tables, especially those with the highest SC/OC estimates, can elucidate the pervasiveness of the relations presented here, but it is already clear that it would be worthwhile to include radar polarization ratios in future asteroid VIS/IR taxonomic classification systems.

Why are E class NEAs so abundant in our sample? The E class is thought to be rare among NEAs (Binzel et al., 2004; Clark et al., 2004), and only $\sim$1% of meteorite falls are aubrites (Lipschutz and Schultz, 2007), thus the fact that $\sim$6% of our sample (with known taxonomic types) belongs to that class is puzzling. Is this a statistical fluke? Due to the EMP spectral degeneracy, we cannot conduct a direct comparison with results from VIS/IR spectroscopy. It seems that E-class NEAs are significantly overrepresented relative to the abundance of aubrite falls, which presumably derive from a similar source. If, as we suspect, many of the unclassified NEAs with high circular polarization ratios turn out to be E class objects, then the apparent discrepancy could be exacerbated.

Perhaps the aubrites are sufficiently fragile that few reach Earth's surface. Or, the flux could vary strongly with diameter, so that comparisons between the meteorite and NEA populations are not meaningful. [On the other hand, the V class objects in our sample constitute $\sim$6% of the sample, a number very similar to the abundance of HED meteorite falls (Lipschutz and Schultz, 2007).] Another possibility, although perhaps remote, is that some other meteorite group might be masquerading as the E-class asteroids. Is there a substantial unrecognized population of E-class near-Earth asteroids?

Please cite this article in press as: Benner, L.A.M., et al. Near-Earth asteroid surface roughness depends on compositional class. Icarus (2008), doi:10.1016/j.icarus.2008.06.010

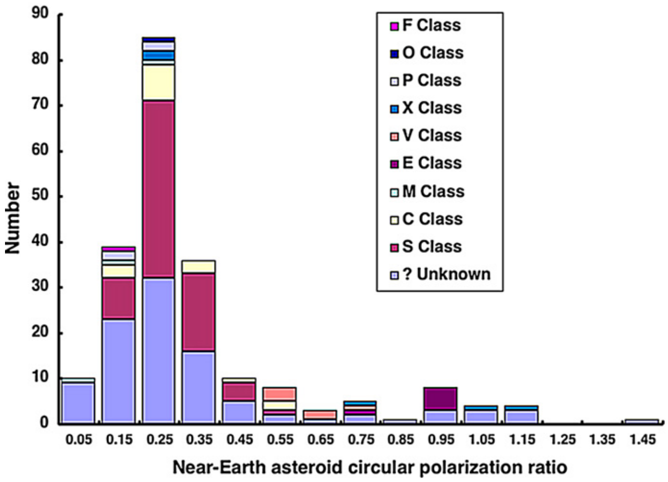

Fig. 3. Histogram of near-Earth asteroid circular polarization ratios broken down by taxonomic class. Bins have widths of 0.1 and are centered on values labeled on the abscissa.

Acknowledgments

We thank the technical staffs at the Arecibo Observatory and the Goldstone Solar System Radar for help with the observations, L.M. Carter for providing the 2004 VG64 data, I.N. Belskaya, R.P. Binzel, S.J. Bus, F. De Meo, M.D. Hicks, and V. Reddy for providing NEA taxonomic classifications in advance of publication, K.G. Ellsworth for help with Fig. 3, and A. Rivkin and B. Campbell for comments that improved the manuscript. The Arecibo Observatory is part of the National Astronomy and Ionosphere Center, which is operated by Cornell University under a cooperative agreement with the National Science Foundation (NSF). Some of this work was performed at the Jet Propulsion Laboratory (JPL), California Institute of Technology, under contract with the National Aeronautics and Space Administration (NASA). This material is based in part upon work supported by NASA under the Science Mission Directorate Research and Analysis Programs.

References

Abe, M., Kitazato, K., Sarugaku, Y., Kawakatsu, Y., Kinoshita, D., 2007. Ground-based observation of post-Hayabusa mission targets. Lunar Planet. Sci. 38, 1638.

Abell, P.A., Gaffey, M.J., Hardersen, P.S., Vilas, F., Jarvis, K.S., Landis, R.R., 2005. Compositions of binary near-Earth objects: Implications for the internal structure of their parent bodies. Bull. Am. Astron. Soc. 37, 627–628.

Abell, P.A., Vilas, F., Reddy, V., Gaffey, M.J., Jarvis, K.S., 2006. Visible and near-infrared spectroscopy of potentially hazardous Asteroid (68950) 2002 QF15. Bull. Am. Astron. Soc. 38, 593.

Barucci, M.A., Fulchignoni, M., Fornasier, S., Dotto, E., Vernazza, P., Birlan, M., Binzel, R.P., Carvano, J., Merlin, F., Barbieri, C., Belskaya, I., 2005. Asteroid target selection for the new Rosetta mission baseline-21 Lutetia and 2867 Steins. Astron. Astrophys. 430, 313–317.

Bell, J.F., Davis, D.R., Hartmann, W.K., Gaffey, M.J., 1989. Asteroids: The big picture. In: Binzel, R.P., Gehrels, T., Matthews, M.S. (Eds.), Asteroids II. Univ. of Arizona Press, Tucson, pp. 921–945.

Benner, L.A.M., and 12 colleagues, 1997. Radar detection of near-Earth Asteroids 2062 Aten, 2101 Adonis, 3103 Eger, 4544 Xanthus, and 1992 QN. Icarus 130, 296–312.

Benner, L.A.M., and 11 colleagues, 1999a. Radar observations of Asteroid 2063 Bacchus. Icarus 139, 309–327.

Benner, L.A.M., Ostro, S.J., Rosema, K.D., Giorgini, J.D., Choate, D., Jurgens, R.F., Rose, R., Slade, M.A., Thomas, M.L., Winkler, R., Yeomans, D.K., 1999b. Radar observations of Asteroid 7822 (1991 CS). Icarus 137, 247–259.

Benner, L.A.M., Ostro, S.J., Hudson, R.S., Rosema, K.D., Jurgens, R.F., Yeomans, D.K., Campbell, D.B., Chandler, J.F., Shapiro, I.I., 2002a. Radar observations of Asteroid 3908 Nyx. Icarus 158, 379–388.

Benner, L.A.M., Ostro, S.J., Nolan, M.C., Margot, J.L., Giorgini, J.D., Hudson, R.S., Jurgens, R.F., Slade, M.A., Howell, E.S., Campbell, D.B., Yeomans, D.K., 2002b. Radar observations of Asteroid 1999 JM8. Meteorit. Planet. Sci. 37, 779–792.

Benner, L.A.M., Nolan, M.C., Margot, J.L., Ostro, S.J., Giorgini, J.D., 2003. Radar imaging of binary near-Earth Asteroid 1998 ST27. Bull. Am. Astron. Soc. 35, 959.

Benner, L.A.M., Nolan, M.C., Ostro, S.J., Giorgini, J.D., Pray, D.P., Harris, A.W., Magri, C., Margot, J.L., 2006a. Near-Earth Asteroid 2005 CR37: Radar images and photometry of a candidate contact binary. Icarus 182, 474–481.

Benner, L.A., Ostro, S.J., Giorgini, J.D., Busch, M.W., Rose, R., Jao, J.S., Jurgens, R.F., 2006b. Radar observations of Asteroid 2004 XP14: An outlier in the near-Earth population. Bull. Am. Astron. Soc. 38, 621.

Binzel, R.P., Rivkin, A.S., Stuart, J.S., Harris, A.W., Bus, S.J., Burbine, T.H., 2004. Observed spectral properties of near-Earth objects: Results for population distribution, source regions, and space weathering processes. Icarus 170, 259–294.

Binzel, R.P., Thomas, C.A., De Meo, F.E., Tokunaga, A., Rivkin, A.S., Bus, S.J., 2006. The MIT–Hawaii–IRTF joint campaign for NEO spectral reconnaissance. Lunar Planet. Sci. 37, 1491.

Binzel, R.P., Rivkin, A.S., Thomas, C.A., Vernazza, P., Burbine, T.H., De Meo, F.E., Bus, S.J., Tokunaga, A.T., Birlan, M., 2007. Spectral properties and composition of potentially hazardous Asteroid (99942) Apophis. Bull. Am. Astron. Soc. 39, 433.

Brozovic, M., Ostro, S.J., Benner, L.A.M., Giorgini, J.D., Jurgens, R.F., Rose, R., Nolan, M.C., Hine, A.A., Magri, C., Scheeres, D.J., Margot, J.L., 2008. Radar observations and a physical model of Asteroid 4660 Nereus, a prime space mission target. Icarus, submitted for publication.

Burbine, T.H., McCoy, T.J., Meibom, A., Gladman, B., Keil, K., 2002. Meteoritic parent bodies: Their number and identification. In: Bottke, W.F., Cellino, A., Binzel, R.P. (Eds.), Asteroids III. Univ. of Arizona Press, Tucson, pp. 653–668.

Bus, S.J., Vilas, F., Barucci, M.A., 2002. Visible-wavelength spectroscopy of asteroids. In: Bottke, W.F., Cellino, A., Binzel, R.P. (Eds.), Asteroids III. Univ. of Arizona Press, Tucson, pp. 169–182.

Busch, M.W., Ostro, S.J., Benner, L.A.M., Giorgini, J.D., Jurgens, R.F., Rose, R., Magri, C., Pravec, P., Scheeres, D.J., Broschart, S.B., 2006. Radar and optical observations and physical modeling of near-Earth Asteroid 10115 (1992 SK). Icarus 181, 145–155.

Busch, M.W., and 16 colleagues, 2007. Physical modeling of near-Earth Asteroid (29075) 1950 DA. Icarus 190, 608–621.

Busch, M.W., Benner, L.A.M., Ostro, S.J., Giorgini, J.D., Jurgens, R.F., Rose, R., Scheeres, D.J., Magri, C., Margot, J.L., Nolan, M.C., Hine, A.A., 2008. Physical properties of near-Earth Asteroid (33342) 1998 WT24. Icarus 195, 614–621.

Campbell, B.A., 2002. Radar Remote Sensing of Planetary Surfaces. Cambridge Univ. Press, Cambridge, UK.

Campbell, B.A., Campbell, D.B., 2006. Regolith properties in the south polar region of the Moon from 70-cm radar polarimetry. Icarus 180, 1–7.

Clark, B.E., Bus, S.J., Rivkin, A.S., McConnochie, T., Sanders, J., Shah, S., Hiroi, T., Shepard, M., 2004. E-type asteroid spectroscopy and compositional modeling. J. Geophys. Res. 109, doi:10.1029/2003JE002200. E02001.

Consolmagno, G.J., Drake, M.J., 1977. Composition and evolution of the eucrite parent body: Evidence from rare Earth elements. Geochim. Cosmochim. Acta 41, 1271–1282.

Cruikshank, D.P., Tholen, D.J., Hartmann, W.K., Bell, J.F., Brown, R.H., 1991. Three basaltic Earth-approaching asteroids and the source of the basaltic meteorites. Icarus 89, 1–13.

Davies, J.K., Harris, A.W., Rivkin, A.S., Wolters, S.D., Green, S.F., McBride, N., Mann, R.K., Kerr, T.H., 2007. Near-infrared spectra of 12 near-Earth objects. Icarus 186, 111–125.

Delbo, M., Harris, A.W., Binzel, R.P., Pravec, P., Davies, J.K., 2003. Keck observations of near-Earth asteroids in the thermal infrared. Icarus 166, 116–130.

Eugster, O., Herzog, G.F., Marti, K., Caffee, M.W., 2006. Irradiation records, cosmic-ray exposure ages, and transfer times of meteorites. In: Lauretta, D.S., McSween, H.Y. (Eds.), Meteorites and the Early Solar System II. Univ. of Arizona Press, Tucson, pp. 829–851.

Fevig, R.A., Fink, U., 2007. Spectral observations of 19 weathered and 23 fresh NEAs and their correlations with orbital parameters. Icarus 188, 175–188.

Fornasier, S., Belskaya, I., Fulchignoni, M., Barucci, M.A., Barbieri, C., 2006. First albedo determination of Asteroid 2867 Steins, target of the *Rosetta* mission. Astron. Astrophys. 449, L9–L12.

Fujiwara, A., and 21 colleagues, 2006. The rubble pile Asteroid Itokawa as observed by Hayabusa. Science 312, 1330–1334.

Gaffey, M.J., Reed, K.L., Kelley, M.S., 1992. Relationship of E-type Apollo Asteroid 3103 (1982 BB) to the enstatite achondrite meteorites and the Hungaria asteroids. Icarus 100, 95–109.

Gietzen, K.M., Lacy, C.H.S., 2007. Visible and near infrared spectra of main belt and near Earth asteroids. Lunar Planet. Sci. 38, 1104.

Giorgini, J.D., Benner, L.A.M., Ostro, S.J., Nolan, M.C., Busch, M.W., 2008. Predicting Earth encounters of (99942) Apophis. Icarus 193, 1–19.

Gradie, J.C., Tedesco, E.F., 1982. Compositional structure of the asteroid belt. Science 216, 1405–1407.

Harmon, J.K., Nolan, M.C., 2005. Radar observations of Comet 2P/Encke during the 2003 apparition. Icarus 176, 175–183.

Harmon, J.K., Campbell, D.B., Hine, A.A., Shapiro, I.I., Marsden, B.G., 1989. Radar observations of Comet IRAS–Araki–Alcock 1983d. Astrophys. J. 338, 1071–1093.

Harmon, J.K., and 15 colleagues, 1997. Radar detection of the nucleus and coma of Comet Hyakutake (C/1996 B2). Science 278, 1921–1924.

Harmon, J.K., Campbell, D.B., Ostro, S.J., Nolan, M.C., 1999. Radar observations of comets. Planet. Space Sci. 47, 1409–1422.
Harmon, J.K., Nolan, M.C., Margot, J.L., Campbell, D.B., Benner, L.A.M., Giorgini, J.D., 2006. Radar observations of Comet P/2005 JQ5 (Catalina). Icarus 184, 285–288.
Harris, A.W., Davies, J.K., Green, S.F., 1998. Thermal infrared spectrophotometry of the near-Earth Asteroids 2100 Ra–Shalom and 1991 EE. Icarus 135, 441–450.
Hicks, M.D., Somers, J., 2007. Physical characterization of radar detected Asteroid 2007 DT103. Bull. Am. Astron. Soc. 39, 433.
Hicks, M.D., Fink, U., Grundy, W.M., 1998. The unusual spectra of 15 near-Earth asteroids and extinct comet candidates. Icarus 133, 69–78.
Howell, E.S., Nolan, M.C., DeRemer, L., Margot, J.L., 2001. Arecibo radar observations of near-Earth Asteroid 2000 EE104. Bull. Am. Astron. Soc. 33, 1153.
Hudson, R.S., and 26 colleagues, 2000. Radar observations and physical model of Asteroid 6489 Golevka. Icarus 148, 37–51.
Hutchison, R., 2006. Meteorites: A Petrologic, Chemical and Isotopic Synthesis. Cambridge Univ. Press, Cambridge, UK.
Kamoun, P., Campbell, D., Pettengill, G., Shapiro, I., 1999. Radar observations of three comets and detection of echoes from one: P/Grigg–Skjellerup. Planet. Space Sci. 47, 23–28.
Kitazato, K., Abe, M., Mito, H., Tarusawa, K., Soyano, T., Nishihara, S., Sarugaku, Y., 2004. Photometric behaviour dependent on solar phase angle and physical characteristics of binary near-Earth Asteroid (65803) 1996 GT. Lunar Planet. Sci. 35, 1623.
Kumar, S., Hardersen, P.S., Gaffey, M.J., 2006. Albedo estimates and near-infrared reflectance spectroscopy of near-Earth Asteroids 1999 HF1 and 2005 AB. Lunar Planet. Sci. 37, 1113.
Lazzarin, M., Marchi, S., Barucci, M.A., Di Martino, M., Barbieri, C., 2004. Visible and near-infrared spectroscopic investigation of near-Earth objects at ESO: First results. Icarus 169, 373–384.
Lazzarin, M., Marchi, S., Magrin, S., Licandro, J., 2005. Spectroscopic investigation of near-Earth objects at Telescopio Nazionale Galileo. Mon. Not. R. Astron. Soc. 359, 1575–1582.
Lipschutz, M.E., Schultz, L., 2007. Meteorites. In: McFadden, L.A., Weissman, P.R., Johnson, T.V. (Eds.), Encyclopedia of the Solar System, second ed. Academic, San Diego, pp. 251–282.
Magri, C., Consolmagno, G.J., Ostro, S.J., Benner, L.A.M., Beeney, B.R., 2001. Radar constraints on asteroid regolith properties using 433 Eros as ground truth. Meteorit. Planet. Sci. 36, 1697–1709.
Magri, C., Nolan, M.C., Ostro, S.J., Giorgini, J.D., 2007a. A radar survey of main-belt asteroids: Arecibo observations of 55 objects during 1999–2003. Icarus 186, 126–151.
Magri, C., Ostro, S.J., Scheeres, D.J., Nolan, M.C., Giorgini, J.D., Benner, L.A.M., Margot, J.L., 2007b. Radar observations and a physical model of Asteroid 1580 Betulia. Icarus 186, 152–177.
Mahapatra, P.R., Ostro, S.J., Benner, L.A.M., Rosema, K.D., Jurgens, R.F., Winkler, R., Rose, R., Giorgini, J.D., Yeomans, D.K., Slade, M.A., 1999. Recent radar observations of Asteroid 1566 Icarus. Planet. Space Sci. 47, 987–995.
Mahapatra, P.R., Benner, L.A.M., Ostro, S.J., Jurgens, R.F., Giorgini, J.D., Yeomans, D.K., Chandler, J.F., Shapiro, I.I., 2002. Radar observations of Asteroid 7335 (1989 JA). Planet. Space Sci. 50, 257–260.
McSween, H.J., 1999. Meteorites and Their Parent Bodies. Cambridge Univ. Press, Cambridge, UK.
Miyamoto, M., and 14 colleagues, 2007. Regolith migration and sorting on Asteroid Itokawa. Science 316, 1011–1014.
Nolan, M.C., Campbell, D.B., Harmon, J.K., Howell, E.S., Magri, C., 2005. Arecibo radar detection of the nucleus and coma of C/2004 Q2 (Maccholz). I. A. U. Symposium 229, 120.
Ostro, S.J., 2007. Planetary radar. In: McFadden, L.A., Weissman, P.R., Johnson, T.V. (Eds.), Encyclopedia of the Solar System, second ed. Academic, San Diego, pp. 735–761.
Ostro, S.J., Campbell, D.B., Shapiro, I.I., 1983. Radar observations of Asteroid 1685 Toro. Astron. J. 88, 565–576.
Ostro, S.J., Yeomans, D.K., Chodas, P.W., Goldstein, R.M., Jurgens, R.F., Thompson, T.W., 1989. Radar observations of Asteroid 1986 JK. Icarus 78, 382–394.
Ostro, S.J., Campbell, D.B., Hine, A.A., Shapiro, I.I., Chandler, J.F., Werner, C.L., Rosema, K.D., 1990. Radar images of Asteroid 1627 Ivar. Astron. J. 99, 2012–2018.
Ostro, S.J., Campbell, D.B., Chandler, J.F., Hine, A.A., Hudson, R.S., Rosema, K.D., Shapiro, I.I., 1991a. Asteroid 1986 DA: Radar evidence for a metallic composition. Science 252, 1399–1404.
Ostro, S.J., Campbell, D.B., Chandler, J.F., Shapiro, I.I., Hine, A.A., Velez, R., Jurgens, R.F., Rosema, K.D., Winkler, R., Yeomans, D.K., 1991b. Asteroid radar astrometry. Astron. J. 102, 1490–1502.
Ostro, S.J., and 12 colleagues, 1996. Radar observations of Asteroid 1620 Geographos. Icarus 121, 46–66.
Ostro, S.J., and 19 colleagues, 1999a. Radar and optical observations of Asteroid 1998 KY26. Science 285, 557–559.
Ostro, S.J., and 15 colleagues, 1999b. Asteroid 4179 Toutatis: 1996 radar observations. Icarus 137, 122–139.
Ostro, S.J., Hudson, R.S., Benner, L.A.M., Nolan, M.C., Giorgini, J.D., Scheeres, D.J., Jurgens, R.F., Rose, R., 2001. Radar observations of Asteroid 1998 ML14. Meteorit. Planet. Sci. 36, 1225–1236.
Ostro, S.J., Hudson, R.S., Benner, L.A.M., Giorgini, J.D., Magri, C., Margot, J.L., Nolan, M.C., 2002. Asteroid radar astronomy. In: Bottke, W.F., Cellino, A., Paolicchi, P., Binzel, R.P. (Eds.), Asteroids III. Univ. of Arizona Press, Tucson, pp. 151–168.
Ostro, S.J., Giorgini, J.D., Benner, L.A.M., Hine, A.A., Nolan, M.C., Margot, J.L., Chodas, P.W., Veillet, C., 2003. Radar detection of Asteroid 2002 AA29. Icarus 166, 271–275.
Ostro, S.J., and 15 colleagues, 2004. Radar observations of Asteroid 25143 Itokawa (1998 SF36). Meteorit. Planet. Sci. 39, 407–424.
Ostro, S.J., and 15 colleagues, 2006. Radar imaging of binary near-Earth Asteroid (66391) 1999 KW4. Science 314, 1276–1280.
Petrovic, J.J., 2001. Mechanical properties of meteorites and their constituents. J. Mater. Sci. 36, 1579–1583.
Pravec, P., Hergenrother, C., Whiteley, R., Sarounova, L., Kusnirak, P., Wolf, M., 2000a. Fast rotating Asteroids 1999 TY2, 1999 SF10, and 1998 WB2. Icarus 147, 477–486.
Pravec, P., and 11 colleagues, 2000b. Slowly rotating Asteroid 1999 GU3. Icarus 148, 589–593.
Pravec, P., and 56 colleagues, 2006. Photometric survey of binary near-Earth asteroids. Icarus 181, 63–93.
Reddy, V., Gaffey, M.J., Hardersen, P.S., Abell, P.A., Kumar, S., 2006. Constraining albedo and composition of potentially-hazardous Asteroids 2004 XP14 and (100085) 1992 UY4 via near-IR spectroscopy. Bull. Am. Astron. Soc. 38, 622.
Rivkin, A.S., Howell, E.S., Vilas, F., Lebofsky, L.A., 2002. Hydrated minerals on asteroids: The astronomical record. In: Bottke, W.F., Cellino, A., Binzel, R.P. (Eds.), Asteroids III. Univ. of Arizona Press, Tucson, pp. 235–253.
Rivkin, A.S., Howell, E.S., Bus, S.J., Hicks, M., Reach, W.T., Jarrett, T.H., Binzel, R.P., 2003. Spectroscopy and photometry of the Earth grazer 2002 NY40. Lunar Planet. Sci. 34, 1722.
Rivkin, A.S., Binzel, R.P., Sunshine, J., Bus, S.J., Burbine, T.H., Saxena, A., 2004. Infrared spectroscopic observations of 69230 Hermes (1937 UB): Possible unweathered endmember among ordinary chondrite analogs. Icarus 172, 408–414.
Rivkin, A.S., Binzel, R.P., Bus, S.J., 2005. Constraining near-Earth object albedos using near-infrared spectroscopy. Icarus 175, 175–180.
Sears, D.W.G., 1995. Enstatite meteorites. In: Shirley, J.H., Fairbridge, R.W. (Eds.), Encyclopedia of Planetary Sciences. Chapman and Hall, London, pp. 234–236.
Shepard, M.K., Benner, L.A.M., Ostro, S.J., Harris, A.W., Rosema, K.D., Shapiro, I.I., Chandler, J.F., Campbell, D.B., 2000. Radar observations of Asteroid 2100 Ra–Shalom. Icarus 147, 520–529.
Shepard, M.K., Benner, L.A.M., Ostro, S.J., Campbell, D.B., Shapiro, I.I., Chandler, J.F., 2004. Radar detection of near-Earth Asteroids 1915 Quetzalcoatl, 3199 Nefertiti, 3757 (1982 XB), and 4034 (1986 PA). Icarus 172, 170–178.
Shepard, M.K., and 13 colleagues, 2006. Radar and infrared observations of binary near-Earth Asteroid 2002 CE26. Icarus 184, 198–210.
Shepard, M.K., and 16 colleagues, 2008a. Multi-wavelength observations of Asteroid 2100 Ra–Shalom. Icarus 193, 20–38.
Shepard, M.K., Kressler, K.M., Clark, B.E., Ockert-Bell, M.E., Nolan, M.C., Howell, E.S., Magri, C., Giorgini, J.D., Benner, L.A.M., Ostro, S.J., 2008b. Radar observations of E-class Asteroids 44 Nysa and 434 Hungaria. Icarus 195, 220–225.
Taylor, P.A., Margot, J.L., Nolan, M.C., Benner, L.A., Ostro, S.J., Giorgini, J.D., Magri, C., 2006. Radar imaging of binary near-Earth Asteroid 2004 DC. Bull. Am. Astron. Soc. 38, 577.
Taylor, P.A., and 11 colleagues, 2007. Spin rate of Asteroid (54509) 2000 PH5 increasing due to the YORP effect. Science 316, 274–277.
Tholen, D.J., 1989. Asteroid taxonomic classifications. In: Binzel, R.P., Gehrels, T., Matthews, M.S. (Eds.), Asteroids II. Univ. of Arizona Press, Tucson, pp. 1139–1161.
Tholen, D.J., Barucci, M.A., 1989. Asteroid taxonomy. In: Binzel, R.P., Gehrels, T., Matthews, M.S. (Eds.), Asteroids II. Univ. of Arizona Press, Tucson, pp. 298–315.
Veverka, J., and 16 colleagues, 1997. NEAR's flyby of 253 Mathilde: Images of a C asteroid. Science 278, 2109–2114.
Volquardsen, E.L., Rivkin, A.S., Bus, S.J., 2007. Composition of hydrated near-Earth object (100085) 1992 UY4. Icarus 187, 464–468.
Wasson, J., 1985. Meteorites: Their Record of Early Solar-System History. W. H. Freeman, New York.
Whiteley, R.J., 2001. A compositional and dynamical survey of the near-Earth asteroids. Ph.D. thesis, University of Hawaii, 202 pp.
Yang, B., Zhu, J., Gao, J., Zhang, J.T., Zhen, X.Z., 2003. Observations of 2000 DP107 in NOAC: Rotation period and reflectance spectrum. Planet. Space Sci. 51, 411–414.
Zellner, B., Leake, M., Morrison, D., Williams, J.G., 1977. The E asteroids and the origin of the enstatite achondrites. Geochim. Cosmochim. Acta 41, 1759–1767.

Please cite this article in press as: Benner, L.A.M., et al. Near-Earth asteroid surface roughness depends on compositional class. Icarus (2008), doi:10.1016/j.icarus.2008.06.010